Mathematical Modelling and testing of the Triangular Biaxial Accelerometers

Xiaowei Shan, Ting Zou, Jorge Angeles, James Richard Forbes

November 28, 2016

Abstract

The multibody-system modelling and simulation of a class of biaxial accelerometers produced with MEMS technology, dubbed *triangular biaxial accelerometers* (TBA), are the subject of this report. The model is obtained using the methodology of the Natural Orthogonal Complement (NOC), in terms of the independent coordinates of the proof-mass displacements and the structural parameters, which is then linearized under the assumption of small-angle rotations of the limbs connecting the proof mass to the accelerometer frame. The simulation results are validated with FEA.

In addition, dimensional optimization and sensitivity analysis is conducted for the TBA structure, which achieves a higher frequency ratio with a lower aspect ratio. The FEA results validate the NOC model, which offers insights into the TBA dynamic behaviour under acceleration fields, for different non-proportional dimensions of the TBA structure.

Keywords: accelerometer; dynamic model; natural orthogonal complement; dimensional optimization; vibration test

1 Introduction

The TBA architecture stems from previous work conducted at McGill University on what was termed Simplicial Biaxial Accelerometers (SBAs) [1, 2], whereby the proof-mass can be any polygon within a frame that follows the shape of the proof-mass. The mathematical model will be derived for the layout shown in Fig. 1, a design proposed by Zou [2].

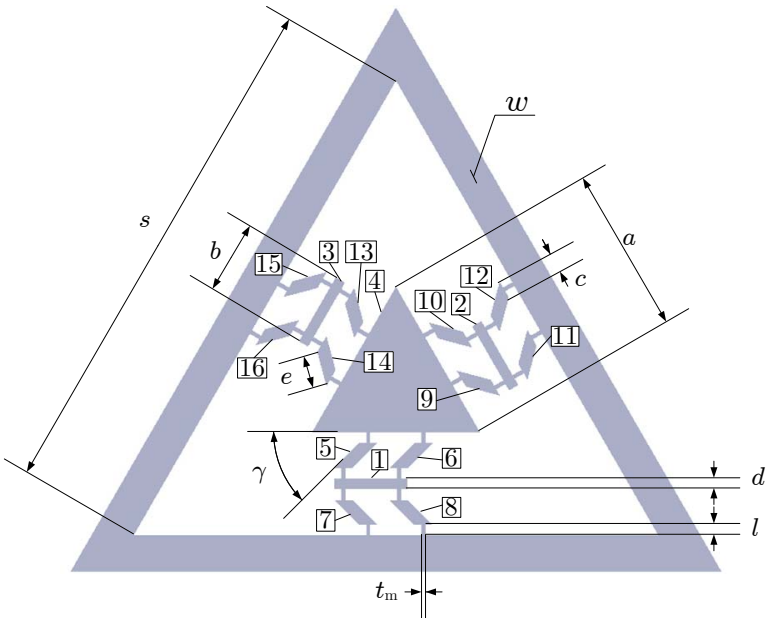

Figure 1: Sketch of the TBA architecture

The accelerometer of Fig. 1 is intended to measure the in-plane acceleration components of the center of mass (c.o.m.) of the triangular proof mass, while filtering the out-of-plane component. To this end, the proof mass is suspended from its frame by means of three identical linkages, termed the *limbs* of the device. Each limb is made of a series array of two parallelogram linkages (PL), which thus allow the proof mass to translate in its plane without rotating. The whole device is fabricated as a compliant mechanism [3]. Because of their shape and their function, the PL are regarded as joints, capable of constraining the motion of two rigid links, one distal, the other proximated to the base, to undergo a relative translation under which every point of one of these two links traces a circle on the other link. In the realm of parallel-kinematics machines (PKM), these parallelogram linkages are termed Π-joints [4–7].

The ΠΠ-limbs [2, 8] of the this TBA architecture shown in Fig. 1 make the assumption reasonable that the proof-mass undergoes pure translation, if the angles of rotation of the limbs of the compliant mechanism are small. To derive the mathematical model, the methodology of the Natural Orthogonal Complement (NOC) is used [9–11], which enables us to express the kinematic constraints as a linear homogeneous system of equations in the vector array of body twist—six-dimensional arrays involving angular and point velocity vectors.

2 Kinematics

Figure 1 serves to illustrate the basic parameters and to identify the rigid bodies composing the TBA. The depth w is measured in the direction normal to the plane of the figure. Numbers are labelled for the rigid-bodies in the following order: the four rigid bodies under pure in-plane translation are numbered 1 to 4, with the bar-shaped rigid-bodies counter-clockwise and the proof-mass as rigid-body 4; the intermediate rigid-bodies, of axes parallel to the sides of the triangles, move under both translation and rotation; these are numbered around the bar-shaped rigid-bodies from left to right and top to bottom.

The coordinate frames introduced to derive the kinematics of the TBA are described below. Let $\mathcal{F}_1$ $\{O, X_1, Y_1, Z_1\}$ be the frame with its origin O located at the centre of the outer frame and its Y_1-axis pointing to vertex R_1; let frames $\mathcal{F}_2$ and $\mathcal{F}_3$ be the counterparts of $\mathcal{F}_1$ with their Y_2- and Y_3-axes pointing to vertices R_2 and R_3, respectively. Because of the periodic symmetry of the accelerometer, the geometric and kinematic relations derived for limb-1 in $\mathcal{F}_1$ are the same as those derived for limbs 2 and 3 in frames $\mathcal{F}_2$ and $\mathcal{F}_3$, respectively. Let $\mathcal{F}_1$ be the base frame.

We define the displacement of the centre of the proof-mass and its time derivative as

$$\boldsymbol{q} \equiv [x_{\rm c}, y_{\rm c}, z_{\rm c}]^{\rm T}, \quad \dot{\boldsymbol{q}} \equiv [\dot{x}_{\rm c}, \dot{y}_{\rm c}, \dot{z}_{\rm c}]^{\rm T}. \tag{1}$$

which are the three independent generalized coordinates and generalized velocities, needed to describe the posture and the gesture, respectively, of the three-dof mechanical system.

The twist $\boldsymbol{t}_i$ of the ith rigid body is given by

$$\boldsymbol{t}_i \equiv \begin{bmatrix} \boldsymbol{\omega}_i \\ \boldsymbol{v}_i \end{bmatrix}, \tag{2}$$

where $\boldsymbol{\omega}_i$ and $\boldsymbol{v}_i$ are, respectively, the angular velocity vector and the velocity vector of the c.o.m. of the ith rigid body in its local frame.

The twists $\boldsymbol{t}_i$ are expressed as linear transformations of $\dot{\boldsymbol{q}}$ in the form

$$\boldsymbol{t}_i = \boldsymbol{T}_i(\boldsymbol{\alpha})\dot{\boldsymbol{q}}, \tag{3}$$

where the 6×3 *twist-shaping matrix* (TSM) $\boldsymbol{T}_i(\boldsymbol{\alpha})$ can be found from the 6-dimensional twist array $\boldsymbol{t}_i$ in terms of the generalized-velocity vector $\dot{\boldsymbol{q}}$. Argument $\boldsymbol{\alpha}$ of the TSM is defined below.

The velocity $\boldsymbol{v}_i$ and the angular velocity $\boldsymbol{\omega}_i$ for each rigid body are derived in terms of $\dot{\boldsymbol{q}}$ and $\boldsymbol{\alpha}$, where $\boldsymbol{\alpha} = [\alpha_1, \alpha_2, \alpha_3, \alpha_4, \alpha_5, \alpha_6, \beta_1, \beta_2, \beta_3]^{\rm T}$, whose components are shown in Fig. 2. Combining these two vectors yields the twist $\boldsymbol{t}_i$ of the ith rigid body, which can be used to find the TSM $\boldsymbol{T}_i(\boldsymbol{\alpha})$. After the TSMs for rigid bodies 4, 1, 5, 6, 7, 8 are obtained, those of the other rigid bodies have the same expressions, as represented in their local frame; then, the TSMs in the reference frame are obtained simply by coordinate transformation.

In Fig. 2, β_2 and β_3 are the out-of-plane angles for the other two $\Pi\Pi$-limbs in the same pattern with β_1. $M_{\rm a1}$ is the midpoint of side Q_2Q_3 of the proof-mass and $M_{\rm s1}$ is the midpoint of side R_2R_3 of the TBA frame; by the same token, $M_{\rm a2}$ is the midpoint of side Q_1Q_3 of the proof-mass, $M_{\rm s2}$ is the midpoint of side R_1R_3 of the TBA frame, and $M_{\rm b2}$ is the midpoint of bar 2; $M_{\rm a3}$ is the midpoint of side Q_1Q_2 of the proof-mass, $M_{\rm s3}$ is the midpoint of side R_1R_2 of the TBA frame,

and $M_{\mathrm{b}3}$ is the midpoint of bar 3. Let h be the distance between $M_{\mathrm{a}i}$ and $M_{\mathrm{b}i}$, which equals the distance between $M_{\mathrm{b}i}$ and M_{si}, for $i = 1, 2, 3$; then, h_α is the projection of h onto the X-Y plane at the home posture and h_β is the projection of h on the Y-Z plane at the home position. Moreover, the out-of-plane displacement is much smaller than its in-plane counterpart, which allows us to write $h_\alpha \approx h$ under the assumption of small rotations of the limbs, i.e., $h = \sqrt{6}(s-a)/12$ and $h_{\mathrm{a}1} = h\sin\alpha_2$, $h_{s1} = h\sin\alpha_1$.

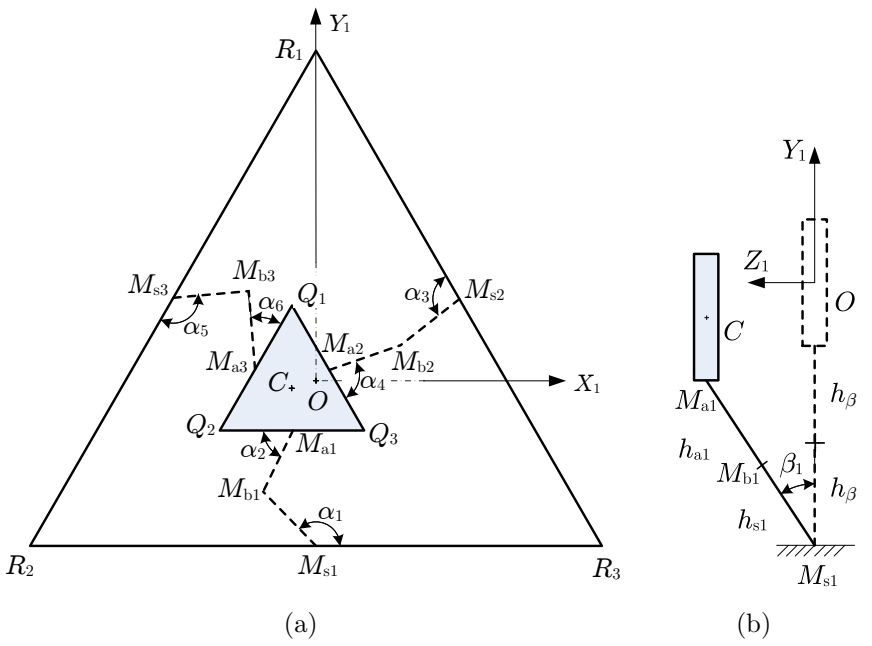

Figure 2: Geometric relations in the TBA: (a) in-plane; (b) out-of-plane

Rigid Body 1

The motion of this body is analyzed in $\mathcal{F}_1$. The rotation matrix from $\mathcal{F}_1$ to $\mathcal{F}$ is the 3×3 identity matrix $\mathbf{1}$. Body-1 undergoes 3D translations and an out-of-plane rotation along the X_1-axis. Hence, the angular velocity of this body is $\boldsymbol{\omega}_1 = \left[\dot{\beta}_1, 0, 0\right]^{\mathrm{T}}$. Subscripted brackets 1 indicate that the array inside is expressed in $\mathcal{F}_1$.

The position vector $\mathbf{c}_1$ in $\mathcal{F}_1$ has the representation

$$[\,\mathbf{c}_1\,]_1 = \begin{bmatrix} h(\cos\alpha_1 + \cos\alpha_2) \\ h(\sin\alpha_1 + \sin\alpha_2) - \dfrac{\sqrt{3}}{6}(s-a) \\ (h_{\mathrm{a}1} + h_{\mathrm{s}1})\sin\beta_1 = h(\sin\alpha_1 + \sin\alpha_2)\sin\beta_1 \end{bmatrix}. \tag{4}$$

The position vectors of $M_{\mathrm{a}1}$ and $M_{\mathrm{s}1}$ are given below:

$$[\boldsymbol{\xi}_{\mathrm{a}1}]_1 = \begin{bmatrix} [x_{\mathrm{c}}]_1 \\ [y_{\mathrm{c}}]_1 - \dfrac{\sqrt{3}}{6}a \\ [z_{\mathrm{c}}]_1 \end{bmatrix}, \quad [\boldsymbol{\xi}_{\mathrm{s}1}]_1 = \begin{bmatrix} 0 \\ -\dfrac{\sqrt{3}}{6}s \\ 0 \end{bmatrix}. \tag{5}$$

The position vector of point $M_{\mathrm{b}1}$ in $\mathcal{F}_1$ is readily obtained as

$$[\boldsymbol{\xi}_1]_1 = [\boldsymbol{\xi}_{\mathrm{s}1}]_1 + \begin{bmatrix} h\cos\alpha_1 \\ h\sin\alpha_1 \\ h_{\mathrm{s}1}\sin\beta_1 \end{bmatrix} = \begin{bmatrix} h\cos\alpha_1 \\ h\sin\alpha_1 - \dfrac{\sqrt{3}}{6}s \\ h\sin\alpha_1\sin\beta_1 \end{bmatrix}. \tag{6}$$

Therefore, the velocity of rigid body 1 is

$$[\boldsymbol{v}_1]_1 = [\dot{\boldsymbol{\xi}}_1]_1 = \begin{bmatrix} -\dot{\alpha}_1 h\sin\alpha_1 \\ \dot{\alpha}_1 h\cos\alpha_1 \\ \dot{\alpha}_1 h\cos\alpha_1\sin\beta_1 + \dot{\beta}_1 h\sin\alpha_1\cos\beta_1 \end{bmatrix}, \tag{7}$$

and the twist $\boldsymbol{t}_1$ becomes

$$[\boldsymbol{t}_1]_1 = \begin{bmatrix} 0 & 0 & 1 \\ 0 & 0 & 0 \\ 0 & 0 & 0 \\ -h\sin\alpha_1 & 0 & 0 \\ h\cos\alpha_1 & 0 & 0 \\ h\cos\alpha_1\sin\beta_1 & 0 & h\sin\alpha_1\cos\beta_1 \end{bmatrix} \begin{bmatrix} \dot{\alpha}_1 \\ \dot{\alpha}_2 \\ \dot{\beta}_1 \end{bmatrix} = \boldsymbol{T}_{01}\dot{\boldsymbol{\alpha}}_1. \tag{8}$$

Moreover, from the geometric relations (4), the time derivatives $\dot{\alpha}_1$, $\dot{\alpha}_2$ and $\dot{\beta}_1$ can be expressed in terms of $\dot{\boldsymbol{q}}$, the velocity array of the proof-mass,i.e., in terms of the generalized velocities, as

$$\dot{\boldsymbol{\alpha}}_1 = \boldsymbol{R}_1 [\dot{\boldsymbol{q}}]_1, \tag{9}$$

where

$$\boldsymbol{R}_1 = \begin{bmatrix} -\dfrac{\cos\alpha_2}{h\sin(\alpha_1-\alpha_2)} & -\dfrac{\sin\alpha_2}{h\sin(\alpha_1-\alpha_2)} & 0 \\ \dfrac{\cos\alpha_1}{h\sin(\alpha_1-\alpha_2)} & \dfrac{\sin\alpha_1}{h\sin(\alpha_1-\alpha_2)} & 0 \\ 0 & -\dfrac{\sin\beta_1}{h\cos\beta_1(\sin\alpha_1+\sin\alpha_2)} & \dfrac{1}{h\cos\beta_1(\sin\alpha_1+\sin\alpha_2)} \end{bmatrix}.$$

Hence, the TSM of rigid body 1 in $\mathcal{F}_1$ is

$$[\boldsymbol{T}_1]_1 = \boldsymbol{T}_{01}\boldsymbol{R}_1. \tag{10}$$

Rigid Body 2

The motion of this body is analyzed in $\mathcal{F}_2$. Let $\boldsymbol{Q}_{21}$ be the 3×3 rotation matrix from $\mathcal{F}_2$ to $\mathcal{F}$, i.e.,

$$\boldsymbol{Q}_{21} = \begin{bmatrix} \cos\left(\frac{2}{3}\pi\right) & -\sin\left(\frac{2}{3}\pi\right) & 0 \\ \sin\left(\frac{2}{3}\pi\right) & \cos\left(\frac{2}{3}\pi\right) & 0 \\ 0 & 0 & 1 \end{bmatrix} = \begin{bmatrix} -\frac{1}{2} & -\frac{\sqrt{3}}{2} & 0 \\ \frac{\sqrt{3}}{2} & -\frac{1}{2} & 0 \\ 0 & 0 & 1 \end{bmatrix}. \tag{11}$$

Since body-2 undergoes pure in-plane translational motion, the angular velocity of this body is $\boldsymbol{\omega}_2 = \begin{bmatrix} \dot{\beta}_2, 0, 0 \end{bmatrix}^{\mathrm{T}}$. From the isotropy of the TBA, the expression of the position vector $\boldsymbol{\xi}_{\mathrm{b}2}$ of point $M_{\mathrm{b}2}$ in $\mathcal{F}_2$ is similar to $\boldsymbol{\xi}_{\mathrm{b}1}$ in $\mathcal{F}_1$, i.e.,

$$[\boldsymbol{\xi}_2]_2 = [\boldsymbol{\xi}_{\mathrm{s}2}]_2 + \begin{bmatrix} h\cos\alpha_3 \\ h\sin\alpha_3 \\ h_{\mathrm{s}2}\sin\beta_2 \end{bmatrix} = \begin{bmatrix} h\cos\alpha_3 \\ h\sin\alpha_3 - \frac{\sqrt{3}}{6}s \\ h\sin\alpha_3\sin\beta_2 \end{bmatrix}, \tag{12}$$

where the bracket with subscript 2 indicates that the vector-components are expressed in $\mathcal{F}_2$. Moreover, $\boldsymbol{\xi}_{\mathrm{s}2}$ is the position vector of $M_{\mathrm{s}2}$.

Therefore, the velocity of rigid body 2 is

$$[\boldsymbol{v}_2]_2 = [\dot{\boldsymbol{\xi}}_2]_2 = \begin{bmatrix} -\dot{\alpha}_3 h\sin\alpha_3 \\ \dot{\alpha}_3 h\cos\alpha_3 \\ \dot{\alpha}_3 h\cos\alpha_3\sin\beta_2 + \dot{\beta}_2 h\sin\alpha_3\cos\beta_2 \end{bmatrix}, \tag{13}$$

and the twist $\boldsymbol{t}_2$ becomes

$$[\boldsymbol{t}_2]_2 = \begin{bmatrix} 0 & 0 & 1 \\ 0 & 0 & 0 \\ 0 & 0 & 0 \\ -h\sin\alpha_3 & 0 & 0 \\ h\cos\alpha_3 & 0 & 0 \\ h\cos\alpha_3\sin\beta_2 & 0 & h\sin\alpha_3\cos\beta_2 \end{bmatrix} \begin{bmatrix} \dot{\alpha}_3 \\ \dot{\alpha}_4 \\ \dot{\beta}_2 \end{bmatrix} = \boldsymbol{T}_{02}\dot{\boldsymbol{\alpha}}_2. \tag{14}$$

Moreover, from the geometric relations (4), the time derivatives $\dot{\alpha}_3$, $\dot{\alpha}_4$ and $\dot{\beta}_2$ can be expressed in terms of $\dot{\boldsymbol{q}}$ as

$$\dot{\boldsymbol{\alpha}}_2 = \boldsymbol{R}_2 \left[\dot{\boldsymbol{q}}\right]_2, \tag{15}$$

where

$$\boldsymbol{R}_2 = \begin{bmatrix} -\dfrac{\cos\alpha_4}{h\sin(\alpha_3-\alpha_4)} & -\dfrac{\sin\alpha_4}{h\sin(\alpha_3-\alpha_4)} & 0 \\ \dfrac{\cos\alpha_3}{h\sin(\alpha_3-\alpha_4)} & \dfrac{\sin\alpha_3}{h\sin(\alpha_3-\alpha_4)} & 0 \\ 0 & -\dfrac{\sin\beta_2}{h\cos\beta_2(\sin\alpha_3+\sin\alpha_4)} & \dfrac{1}{h\cos\beta_2(\sin\alpha_3+\sin\alpha_4)} \end{bmatrix}.$$

Hence, the TSM of rigid body 2 in $\mathcal{F}_2$ is

$$[\boldsymbol{T}_2]_2 = \boldsymbol{T}_{02}\boldsymbol{R}_2. \tag{16}$$

Rigid Body 3

The motion of this body is analyzed in $\mathcal{F}_3$. Let $\boldsymbol{Q}_{31}$ be the 3×3 rotation matrix from $\mathcal{F}_3$ to $\mathcal{F}$, i.e.,

$$\boldsymbol{Q}_{31} = \begin{bmatrix} \cos\left(-\frac{2}{3}\pi\right) & -\sin\left(-\frac{2}{3}\pi\right) & 0 \\ \sin\left(-\frac{2}{3}\pi\right) & \cos\left(-\frac{2}{3}\pi\right) & 0 \\ 0 & 0 & 1 \end{bmatrix} = \begin{bmatrix} -\frac{1}{2} & \frac{\sqrt{3}}{2} & 0 \\ -\frac{\sqrt{3}}{2} & -\frac{1}{2} & 0 \\ 0 & 0 & 1 \end{bmatrix}. \tag{17}$$

Since body-3 undergoes pure in-plane translational motion, the angular velocity of this body is $\boldsymbol{\omega}_3 = \begin{bmatrix}\dot\beta_3, 0, 0\end{bmatrix}^{\mathrm{T}}$. From the isotropy of the TBA, the expression of the position vector $\boldsymbol{\xi}_{\mathrm{b}3}$ of point $M_{\mathrm{b}3}$ in $\mathcal{F}_3$ is similar to $\boldsymbol{\xi}_{\mathrm{b}1}$ in $\mathcal{F}_1$, i.e.,

$$[\boldsymbol{\xi}_3]_3 = [\boldsymbol{\xi}_{\mathrm{s}3}]_3 + \begin{bmatrix} h\cos\alpha_5 \\ h\sin\alpha_5 \\ h_{\mathrm{s}3}\sin\beta_3 \end{bmatrix} = \begin{bmatrix} h\cos\alpha_5 \\ h\sin\alpha_5 - \dfrac{\sqrt{3}}{6}s \\ h\sin\alpha_5\sin\beta_3 \end{bmatrix}, \tag{18}$$

where the bracket with subscript 3 indicates that the vector-components are expressed in $\mathcal{F}_3$. Moreover, $\boldsymbol{\xi}_{\mathrm{s}3}$ is the position vector of $M_{\mathrm{s}3}$.

Therefore, the velocity of rigid body 3 is

$$[\boldsymbol{v}_3]_3 = [\dot{\boldsymbol{\xi}}_3]_3 = \begin{bmatrix} -\dot\alpha_5 h\sin\alpha_5 \\ \dot\alpha_5 h\cos\alpha_5 \\ \dot\alpha_5 h\cos\alpha_5\sin\beta_3 + \dot\beta_3 h\sin\alpha_5\cos\beta_3 \end{bmatrix}, \tag{19}$$

and the twist $\boldsymbol{t}_3$ becomes

$$[\boldsymbol{t}_3]_3 = \begin{bmatrix} 0 & 0 & 1 \\ 0 & 0 & 0 \\ 0 & 0 & 0 \\ -h\sin\alpha_5 & 0 & 0 \\ h\cos\alpha_5 & 0 & 0 \\ h\cos\alpha_5\sin\beta_3 & 0 & h\sin\alpha_5\cos\beta_3 \end{bmatrix} \begin{bmatrix} \dot{\alpha}_5 \\ \dot{\alpha}_6 \\ \dot{\beta}_3 \end{bmatrix} = \boldsymbol{T}_{03}\dot{\boldsymbol{\alpha}}_3, \tag{20}$$

Moreover, from the geometric relations (4), the time derivatives $\dot{\alpha}_5$, $\dot{\alpha}_6$ and $\dot{\beta}_3$ can be expressed in terms of $\dot{\boldsymbol{q}}$ as

$$\dot{\boldsymbol{\alpha}}_3 = \boldsymbol{R}_3 \left[\dot{\boldsymbol{q}}\right]_3, \tag{21}$$

where

$$\boldsymbol{R}_3 = \begin{bmatrix} -\dfrac{\cos\alpha_6}{h\sin(\alpha_5-\alpha_6)} & -\dfrac{\sin\alpha_6}{h\sin(\alpha_5-\alpha_6)} & 0 \\ \dfrac{\cos\alpha_5}{h\sin(\alpha_5-\alpha_6)} & \dfrac{\sin\alpha_5}{h\sin(\alpha_5-\alpha_6)} & 0 \\ 0 & -\dfrac{\sin\beta_3}{h\cos\beta_3(\sin\alpha_5+\sin\alpha_6)} & \dfrac{1}{h\cos\beta_3(\sin\alpha_5+\sin\alpha_6)} \end{bmatrix}.$$

Hence, the TSM of rigid body 3 in $\mathcal{F}_3$ is

$$[\boldsymbol{T}_3]_3 = \boldsymbol{T}_{03}\boldsymbol{R}_3. \tag{22}$$

Rigid Body 4

Rigid body 4, the proof-mass, is analyzed in the reference frame $\mathcal{F}$. Since body 4 undergoes pure translational motion in and out of the plane, the angular velocity of this body is $\boldsymbol{\omega_4} = \boldsymbol{0}_{3\times1}$. The expression of the position vector $\boldsymbol{\xi}_4$ in $\mathcal{F}$ is

$$\boldsymbol{\xi}_4 = \begin{bmatrix} x_c \\ y_c \\ z_c \end{bmatrix} = \boldsymbol{q}. \tag{23}$$

Therefore, the velocity of rigid body 4 is

$$\boldsymbol{v}_4 = \dot{\boldsymbol{q}}, \tag{24}$$

and the twist $\boldsymbol{t}_4$ becomes

$$\boldsymbol{t}_4 = \begin{bmatrix} \boldsymbol{0}_{3\times3} \\ \boldsymbol{1}_{3\times3} \end{bmatrix} \dot{\boldsymbol{q}} = \boldsymbol{T}_4\dot{\boldsymbol{q}}. \tag{25}$$

Rigid Body 5

Let $\phi,\ \theta,\ \psi$ be the small angles of rotation in the roll, pitch, yaw direction, respectively. Rigid body 5 is analyzed in $\mathcal{F}_1$. The angles of rotation of body 5 are

$$\phi_5 = \beta_1, \quad \theta_5 = 0, \quad \psi_5 = \alpha_2 - \gamma. \tag{26}$$

Since γ is constant, the angular velocity $\boldsymbol{\omega}_5$ of body 5 is

$$\boldsymbol{\omega}_5 = \left[\dot{\phi}_5, \dot{\theta}_5, \dot{\psi}_5\right] = \left[\dot{\beta}_1, 0, \dot{\alpha}_2\right]^{\mathrm{T}}. \tag{27}$$

The position vector $\boldsymbol{\xi}_5$ derived from the geometric relation shown in Fig. 2 is given as

$$\begin{aligned}
[\boldsymbol{\xi}_5]_1 &= [\boldsymbol{\xi}_{\mathrm{b1}}]_1 + \frac{1}{2}([\boldsymbol{\xi}_{\mathrm{a1}}]_1 - [\boldsymbol{\xi}_{\mathrm{b1}}]_1) - \left[\frac{b-c}{2}, 0, 0\right]^{\mathrm{T}} + \left[\frac{d}{4} + l, \frac{d}{4}, 0\right]^{\mathrm{T}} \\
&= \frac{1}{2}\begin{bmatrix} h\cos\alpha_1 + [x_{\mathrm{c}}]_1 - b + c + d/2 + 2l \\ h\sin\alpha_1 + [y_{\mathrm{c}}]_1 - \dfrac{\sqrt{3}}{6}(s+a) + d/2 \\ h\sin\alpha_1\sin\beta_1 + [z_{\mathrm{c}}]_1 \end{bmatrix},
\end{aligned} \tag{28}$$

in which the last two terms of the first row compensate the deviations caused by the geometric simplification of the ΠΠ-limb.

Therefore, the velocity of body 5 is

$$[\boldsymbol{v}_5]_1 = [\dot{\boldsymbol{\xi}}_5]_1 = \begin{bmatrix} -\dot{\alpha}_1 h\sin\alpha_1 - \dfrac{1}{2}\dot{\alpha}_2 h\sin\alpha_2 \\ \dot{\alpha}_1 h\cos\alpha_1 + \dfrac{1}{2}\dot{\alpha}_2 h\cos\alpha_2 \\ \dot{\alpha}_1 h\cos\alpha_1\sin\beta_1 + \dfrac{1}{2}\dot{\alpha}_2 h\cos\alpha_2\sin\beta_1 + \dot{\beta}_1 h\cos\beta_1\left(\sin\alpha_1 + \dfrac{1}{2}\sin\alpha_2\right) \end{bmatrix}, \tag{29}$$

and the twist $\boldsymbol{t}_5$ becomes

$$[\boldsymbol{t}_5]_1 = \begin{bmatrix} 0 & 0 & 1 \\ 0 & 0 & 0 \\ 0 & 1 & 0 \\ -h\sin\alpha_1 & -\dfrac{1}{2}h\sin\alpha_2 & 0 \\ h\cos\alpha_1 & \dfrac{1}{2}h\cos\alpha_2 & 0 \\ h\cos\alpha_1\sin\beta_1 & \dfrac{1}{2}h\cos\alpha_2\sin\beta_1 & h\cos\beta_1\left(\sin\alpha_1 + \dfrac{1}{2}\sin\alpha_2\right) \end{bmatrix} \begin{bmatrix} \dot{\alpha}_1 \\ \dot{\alpha}_2 \\ \dot{\beta}_1 \end{bmatrix} = \boldsymbol{T}_{05}\dot{\boldsymbol{\alpha}}_1. \tag{30}$$

Hence, the TSM of body-5 in $\mathcal{F}_1$ is

$$[\boldsymbol{T}_5]_1 = \boldsymbol{T}_{05}\boldsymbol{R}_1. \tag{31}$$

Rigid Body 6

Similar to rigid body 5, the angular velocity of body 6 is

$$\boldsymbol{\omega}_6 = \boldsymbol{\omega}_5. \tag{32}$$

The position vector $\boldsymbol{\xi}_6$ derived from the geometric relation shown in Fig. 2 is given as

$$\begin{aligned}[\boldsymbol{\xi}_6]_1 &= [\boldsymbol{\xi}_{\mathrm{b}1}]_1 + \frac{1}{2}([\boldsymbol{\xi}_{\mathrm{a}1}]_1 - [\boldsymbol{\xi}_{\mathrm{b}1}]_1) + \left[\frac{b-c}{2}, 0, 0\right]^{\mathrm{T}} + \left[\frac{d}{4} + l, \frac{d}{4}, 0\right]^{\mathrm{T}} \\ &= \frac{1}{2}\begin{bmatrix} h\cos\alpha_1 + [x_{\mathrm{c}}]_1 + b - c + d/2 + 2l \\ h\sin\alpha_1 + [y_{\mathrm{c}}]_1 - \dfrac{\sqrt{3}}{6}(s+a) + d/2 \\ h\sin\alpha_1\sin\beta_1 + [z_{\mathrm{c}}]_1 \end{bmatrix}.\end{aligned} \tag{33}$$

Therefore, the velocity of body 6 is

$$[\boldsymbol{v}_6]_1 = [\dot{\boldsymbol{\xi}}_6]_1 = [\boldsymbol{v}_5]_1, \tag{34}$$

the twist $\boldsymbol{t}_6$ and the TSM $\boldsymbol{T}_6$ of body 6 in $\mathcal{F}_1$ then being

$$[\boldsymbol{t}_6]_1 = [\boldsymbol{t}_5]_1, \quad [\boldsymbol{T}_6]_1 = [\boldsymbol{T}_5]_1 = \boldsymbol{T}_{05}\boldsymbol{R}_1. \tag{35}$$

Rigid Body 7

Rigid body 7 is analyzed in $\mathcal{F}_1$. The angles of rotation of body 7 are

$$\phi_5 = \beta_1, \quad \theta_7 = 0, \quad \psi_7 = \alpha_1 - (\pi - \gamma). \tag{36}$$

The angular velocity of body 7 is

$$\boldsymbol{\omega}_7 = \left[\dot{\phi}_7, \dot{\theta}_7, \dot{\psi}_7\right] = \left[\dot{\beta}_1, 0, \dot{\alpha}_1\right]^{\mathrm{T}}. \tag{37}$$

The position vector $\boldsymbol{\xi}_7$ derived from the geometric relation shown in Fig. 2 is given as

$$\begin{aligned}[\boldsymbol{\xi}_7]_1 &= [\boldsymbol{\xi}_{\mathrm{s}1}]_1 + \frac{1}{2}([\boldsymbol{\xi}_{\mathrm{b}1}]_1 - [\boldsymbol{\xi}_{\mathrm{s}1}]_1) - \left[\frac{b-c}{2}, 0, 0\right]^{\mathrm{T}} + \left[\frac{d}{4} + l, -\frac{d}{4}, 0\right]^{\mathrm{T}} \\ &= \frac{1}{2}\begin{bmatrix} h\cos\alpha_1 - b + c + d/2 + 2l \\ h\sin\alpha_1 - \dfrac{\sqrt{3}}{3}s - d/2 \\ h\sin\alpha_1\sin\beta_1 \end{bmatrix}.\end{aligned} \tag{38}$$

Therefore, the velocity of body 7 is

$$[\boldsymbol{v}_7]_1 = [\dot{\boldsymbol{\xi}}_7]_1 = \frac{1}{2}\begin{bmatrix} -\dot{\alpha}_1 h\sin\alpha_1 \\ \dot{\alpha}_1 h\cos\alpha_1 \\ \dot{\alpha}_1 h\cos\alpha_1\sin\beta_1 + \dot{\beta}_1 h\sin\alpha_1\cos\beta_1 \end{bmatrix}, \tag{39}$$

and the twist $\boldsymbol{t}_7$ becomes

$$[\boldsymbol{t}_7]_1 = \begin{bmatrix} 0 & 0 & 1 \\ 0 & 0 & 0 \\ 1 & 0 & 0 \\ -\frac{1}{2}h\sin\alpha_1 & 0 & 0 \\ \frac{1}{2}h\cos\alpha_1 & 0 & 0 \\ \frac{1}{2}h\cos\alpha_1\sin\beta_1 & 0 & \frac{1}{2}h\sin\alpha_1\cos\beta_1 \end{bmatrix} \begin{bmatrix} \dot{\alpha}_1 \\ \dot{\alpha}_2 \\ \dot{\beta}_1 \end{bmatrix} = \boldsymbol{T}_{07}\dot{\boldsymbol{\alpha}}_1. \tag{40}$$

Hence, the TSM of body-7 in $\mathcal{F}_1$ is

$$[\boldsymbol{T}_7]_1 = \boldsymbol{T}_{07}\boldsymbol{R}_1. \tag{41}$$

Rigid Body 8

Similar to rigid body 7, the angular velocity of rigid body 8 is

$$\boldsymbol{\omega}_8 = \boldsymbol{\omega}_7. \tag{42}$$

The position vector $\boldsymbol{\xi}_8$ derived from the geometric relation shown in Fig. 2 is given as

$$\begin{aligned} [\boldsymbol{\xi}_8]_1 &= [\boldsymbol{\xi}_{s1}]_1 + \frac{1}{2}([\boldsymbol{\xi}_{b1}]_1 - [\boldsymbol{\xi}_{s1}]_1) + \left[\frac{b-c}{2}, 0, 0\right]^{\mathrm{T}} + \left[\frac{d}{4} + l, -\frac{d}{4}, 0\right]^{\mathrm{T}} \\ &= \frac{1}{2}\begin{bmatrix} h\cos\alpha_1 + b - c + d/2 + 2l \\ h\sin\alpha_1 - \frac{\sqrt{3}}{3}s - d/2 \\ h\sin\alpha_1\sin\beta_1 \end{bmatrix}. \end{aligned} \tag{43}$$

Therefore, the velocity of body 8 is

$$[\boldsymbol{v}_8]_1 = [\dot{\boldsymbol{\xi}}_8]_1 = [\boldsymbol{v}_7]_1, \tag{44}$$

and the twist $\boldsymbol{t}_8$ and the TSM $\boldsymbol{T}_8$ of body 8 in $\mathcal{F}_1$ are

$$[\boldsymbol{t}_8]_1 = [\boldsymbol{t}_7]_1, \quad [\boldsymbol{T}_8]_1 = [\boldsymbol{T}_7]_1 = \boldsymbol{T}_{07}\boldsymbol{R}_1. \tag{45}$$

Rigid Body 9

The motion of this body is analyzed in $\mathcal{F}_2$. Similar to rigid body 5, the angles of rotation of body 9 are

$$\phi_9 = \beta_2, \quad \theta_9 = 0, \quad \psi_9 = \alpha_4 - \gamma. \tag{46}$$

The angular velocity of body-9 is

$$\boldsymbol{\omega}_9 = \left[\dot{\phi}_9, \dot{\theta}_9, \dot{\psi}_9\right] = \left[\dot{\beta}_2, 0, \dot{\alpha}_4\right]^{\mathrm{T}}. \tag{47}$$

From the isotropy feature of the TBA, the expression for the position vector $\boldsymbol{\xi}_9$ in $\mathcal{F}_2$ is similar to $\boldsymbol{\xi}_5$ in $\mathcal{F}_1$, i.e.,

$$\begin{aligned}[\boldsymbol{\xi}_9]_2 &= [\boldsymbol{\xi}_{\mathrm{b}2}]_2 + \frac{1}{2}([\boldsymbol{\xi}_{\mathrm{a}2}]_2 - [\boldsymbol{\xi}_{\mathrm{b}2}]_2) - \left[\frac{b-c}{2}, 0, 0\right]^{\mathrm{T}} + \left[\frac{d}{4} + l, \frac{d}{4}, 0\right]^{\mathrm{T}} \\ &= \frac{1}{2}\begin{bmatrix} h\cos\alpha_3 + [x_{\mathrm{c}}]_2 - b + c + d/2 + 2l \\ h\sin\alpha_3 + [y_{\mathrm{c}}]_2 - \dfrac{\sqrt{3}}{6}(s+a) + d/2 \\ h\sin\alpha_3\sin\beta_2 + [z_{\mathrm{c}}]_2 \end{bmatrix},\end{aligned} \tag{48}$$

where $\boldsymbol{\xi}_{\mathrm{a}2}$ is the position vector of $M_{\mathrm{a}2}$.

Therefore, the velocity of body 9 is

$$[\boldsymbol{v}_9]_2 = \begin{bmatrix} -\dot{\alpha}_3 h\sin\alpha_3 - \dfrac{1}{2}\dot{\alpha}_4 h\sin\alpha_4 \\ \dot{\alpha}_3 h\cos\alpha_3 + \dfrac{1}{2}\dot{\alpha}_4 h\cos\alpha_4 \\ \dot{\alpha}_3 h\cos\alpha_3\sin\beta_2 + \dfrac{1}{2}\dot{\alpha}_4 h\cos\alpha_4\sin\beta_2 + \dot{\beta}_2 h\cos\beta_2\left(\sin\alpha_3 + \dfrac{1}{2}\sin\alpha_4\right) \end{bmatrix}, \tag{49}$$

and the twist $\boldsymbol{t}_9$ becomes

$$[\boldsymbol{t}_9]_2 = \begin{bmatrix} 0 & 0 & 1 \\ 0 & 0 & 0 \\ 0 & 1 & 0 \\ -h\sin\alpha_3 & -\dfrac{1}{2}h\sin\alpha_4 & 0 \\ h\cos\alpha_3 & \dfrac{1}{2}h\cos\alpha_4 & 0 \\ h\cos\alpha_3\sin\beta_2 & \dfrac{1}{2}h\cos\alpha_4\sin\beta_2 & h\cos\beta_2\left(\sin\alpha_3 + \dfrac{1}{2}\sin\alpha_4\right) \end{bmatrix} \begin{bmatrix} \dot{\alpha}_3 \\ \dot{\alpha}_4 \\ \dot{\beta}_2 \end{bmatrix} = \boldsymbol{T}_{09}\dot{\boldsymbol{\alpha}}_2. \tag{50}$$

Hence, the TSM of body 9 in $\mathcal{F}_2$ is

$$[\boldsymbol{T}_9]_2 = \boldsymbol{T}_{09}\boldsymbol{R}_2. \tag{51}$$

Rigid Body 10

The motion of this body is analyzed in $\mathcal{F}_2$. Similar to rigid body 9, the angular velocity of body 10 is

$$\boldsymbol{\omega}_{10} = \boldsymbol{\omega}_9. \tag{52}$$

The position vector $\boldsymbol{\xi}_{10}$ in $\mathcal{F}_2$ is

$$\begin{aligned}[\boldsymbol{\xi}_{10}]_2 &= [\boldsymbol{\xi}_{\mathrm{b}2}]_2 + \frac{1}{2}([\boldsymbol{\xi}_{\mathrm{a}2}]_2 - [\boldsymbol{\xi}_{\mathrm{b}2}]_2) + \left[\frac{b-c}{2}, 0, 0\right]^{\mathrm{T}} + \left[\frac{d}{4}+l, \frac{d}{4}, 0\right]^{\mathrm{T}} \\ &= \frac{1}{2}\begin{bmatrix} h\cos\alpha_3 + [x_{\mathrm{c}}]_2 + b - c + d/2 + 2l \\ h\sin\alpha_3 + [y_{\mathrm{c}}]_2 - \dfrac{\sqrt{3}}{6}(s+a) + d/2 \\ h\sin\alpha_3\sin\beta_2 + [z_{\mathrm{c}}]_2 \end{bmatrix}.\end{aligned} \tag{53}$$

Therefore, the velocity of body 10 is

$$[\boldsymbol{v}_{10}]_2 = [\boldsymbol{v}_9]_2, \tag{54}$$

and the twist $\boldsymbol{t}_{10}$ and the TSM $\boldsymbol{T}_{10}$ of body-10 in $\mathcal{F}_2$ are

$$[\boldsymbol{t}_{10}]_2 = [\boldsymbol{t}_9]_2, \quad [\boldsymbol{T}_{10}]_2 = [\boldsymbol{T}_9]_2 = \boldsymbol{T}_{09}\boldsymbol{R}_2. \tag{55}$$

Rigid Body 11

The motion of this body is analyzed in $\mathcal{F}_2$. Similar to rigid body 7, The angles of rotation of body 11 are

$$\phi_{11} = \beta_2, \quad \theta_{11} = 0, \quad \psi_{11} = \alpha_3 - (\pi - \gamma). \tag{56}$$

The angular velocity of body 11 is

$$\boldsymbol{\omega}_{11} = \left[\dot{\phi}_{11}, \dot{\theta}_{11}, \dot{\psi}_{11}\right] = \left[\dot{\beta}_2, 0, \dot{\alpha}_3\right]^{\mathrm{T}}. \tag{57}$$

The position vector $\boldsymbol{\xi}_{11}$ derived from the geometric relation shown in Fig. 2 is given as

$$\begin{aligned}[\boldsymbol{\xi}_{11}]_2 &= [\boldsymbol{\xi}_{\mathrm{s}2}]_2 + \frac{1}{2}([\boldsymbol{\xi}_{\mathrm{b}2}]_2 - [\boldsymbol{\xi}_{\mathrm{s}2}]_2) - \left[\frac{b-c}{2}, 0, 0\right]^{\mathrm{T}} + \left[\frac{d}{4}+l, -\frac{d}{4}, 0\right]^{\mathrm{T}} \\ &= \frac{1}{2}\begin{bmatrix} h\cos\alpha_3 - b + c + d/2 + 2l \\ h\sin\alpha_3 - \dfrac{\sqrt{3}}{3}s - d/2 \\ h\sin\alpha_3\sin\beta_2 \end{bmatrix}.\end{aligned} \tag{58}$$

Therefore, the velocity of body 11 is

$$[\boldsymbol{v}_{11}]_2 = [\dot{\boldsymbol{\xi}}_{11}]_2 = \frac{1}{2}\begin{bmatrix} -\dot{\alpha}_3 h\sin\alpha_3 \\ \dot{\alpha}_3 h\cos\alpha_3 \\ \dot{\alpha}_3 h\cos\alpha_3\sin\beta_2 + \dot{\beta}_2 h\sin\alpha_3\cos\beta_2 \end{bmatrix}, \tag{59}$$

and the twist $\boldsymbol{t}_{11}$ becomes

$$[\boldsymbol{t}_{11}]_2 = \begin{bmatrix} 0 & 0 & 1 \\ 0 & 0 & 0 \\ 1 & 0 & 0 \\ -\frac{1}{2}h\sin\alpha_3 & 0 & 0 \\ \frac{1}{2}h\cos\alpha_3 & 0 & 0 \end{bmatrix} \begin{bmatrix} \dot{\alpha}_3 \\ \dot{\alpha}_4 \\ \dot{\beta}_2 \end{bmatrix} = \boldsymbol{T}_{011}\dot{\boldsymbol{\alpha}}_2. \tag{60}$$

Hence, the TSM of body 11 in $\mathcal{F}_2$ is

$$[\boldsymbol{T}_{11}]_2 = \boldsymbol{T}_{011}\boldsymbol{R}_2. \tag{61}$$

Rigid body 12

Similar to rigid body 11, the angular velocity of rigid body 12 is

$$\boldsymbol{\omega}_{12} = \boldsymbol{\omega}_{11}. \tag{62}$$

The position vector $\boldsymbol{\xi}_{12}$ derived from the geometric relation shown in Fig. 2 is given as

$$\begin{aligned} [\boldsymbol{\xi}_{12}]_1 &= [\boldsymbol{\xi}_{s2}]_2 + \frac{1}{2}([\boldsymbol{\xi}_{b2}]_2 - [\boldsymbol{\xi}_{s2}]_2) + \left[\frac{b-c}{2}, 0, 0\right]^{\mathrm{T}} + \left[\frac{d}{4} + l, -\frac{d}{4}, 0\right]^{\mathrm{T}} \\ &= \frac{1}{2}\begin{bmatrix} h\cos\alpha_3 + b - c + d/2 + 2l \\ h\sin\alpha_3 - \dfrac{\sqrt{3}}{3}s - d/2 \\ h\sin\alpha_3\sin\beta_2 \end{bmatrix}. \end{aligned} \tag{63}$$

Therefore, the velocity of body 12 is

$$[\boldsymbol{v}_{12}]_2 = [\boldsymbol{v}_{11}]_2, \tag{64}$$

and the twist $\boldsymbol{t}_{12}$ and the TSM $\boldsymbol{T}_{12}$ of body 12 in $\mathcal{F}_2$ are

$$[\boldsymbol{t}_{12}]_2 = [\boldsymbol{t}_{11}]_2, \quad [\boldsymbol{T}_{12}]_2 = [\boldsymbol{T}_{11}]_2 = \boldsymbol{T}_{011}\boldsymbol{R}_2. \tag{65}$$

Rigid Body 13

The motion of this body is analyzed in $\mathcal{F}_3$. Similar to rigid body 5, the angles of rotation of body-13 are

$$\phi_{13} = \beta_3, \quad \theta_{13} = 0, \quad \psi_{13} = \alpha_6 - \gamma. \tag{66}$$

The angular velocity of body-13 is

$$\boldsymbol{\omega}_{13} = \left[\dot{\phi}_{13}, \dot{\theta}_{13}, \dot{\psi}_{13}\right] = \left[\dot{\beta}_3, 0, \dot{\alpha}_6\right]^{\mathrm{T}}. \tag{67}$$

From the isotropy of the TBA, the expression of the position vector $\boldsymbol{\xi}_{13}$ in $\mathcal{F}_3$ is similar to $\boldsymbol{\xi}_5$ in $\mathcal{F}_1$, i.e.

$$\begin{aligned}[\boldsymbol{\xi}_{13}]_3 &= [\boldsymbol{\xi}_{\mathrm{b}3}]_3 + \frac{1}{2}([\boldsymbol{\xi}_{\mathrm{a}3}]_3 - [\boldsymbol{\xi}_{\mathrm{b}3}]_3) - \left[\frac{b-c}{2}, 0, 0\right]^{\mathrm{T}} + \left[\frac{d}{4}+l, \frac{d}{4}, 0\right]^{\mathrm{T}} \\ &= \frac{1}{2}\begin{bmatrix} h\cos\alpha_5 + [x_{\mathrm{c}}]_3 - b + c + d/2 + 2l \\ h\sin\alpha_5 + [y_{\mathrm{c}}]_3 - \dfrac{\sqrt{3}}{6}(s+a) + d/2 \\ h\sin\alpha_5\sin\beta_3 + [z_{\mathrm{c}}]_3 \end{bmatrix},\end{aligned} \tag{68}$$

where $\boldsymbol{\xi}_{\mathrm{a}3}$ is the position vector of $M_{\mathrm{a}3}$.

Therefore, the velocity of body 9 is

$$[\boldsymbol{v}_{13}]_3 = \begin{bmatrix} -\dot{\alpha}_5 h\sin\alpha_5 - \dfrac{1}{2}\dot{\alpha}_6 h\sin\alpha_6 \\ \dot{\alpha}_5 h\cos\alpha_5 + \dfrac{1}{2}\dot{\alpha}_6 h\cos\alpha_6 \\ \dot{\alpha}_5 h\cos\alpha_5\sin\beta_3 + \dfrac{1}{2}\dot{\alpha}_6 h\cos\alpha_6\sin\beta_3 + \dot{\beta}_3 h\cos\beta_3\left(\sin\alpha_5 + \dfrac{1}{2}\sin\alpha_6\right) \end{bmatrix}, \tag{69}$$

and the twist $\boldsymbol{t}_{13}$ becomes

$$[\boldsymbol{t}_{13}]_3 = \begin{bmatrix} 0 & 0 & 1 \\ 0 & 0 & 0 \\ 0 & 1 & 0 \\ -h\sin\alpha_5 & -\dfrac{1}{2}h\sin\alpha_6 & \\ h\cos\alpha_5 & \dfrac{1}{2}h\cos\alpha_6 & \\ h\cos\alpha_5\sin\beta_3 & \dfrac{1}{2}h\cos\alpha_6\sin\beta_3 & h\cos\beta_3\left(\sin\alpha_5 + \dfrac{1}{2}\sin\alpha_6\right) \end{bmatrix} \begin{bmatrix} \dot{\alpha}_5 \\ \dot{\alpha}_6 \\ \dot{\beta}_3 \end{bmatrix} = \boldsymbol{T}_{013}\dot{\boldsymbol{\alpha}}_3. \tag{70}$$

Hence, the TSM of body 13 in $\mathcal{F}_3$ is

$$[\boldsymbol{T}_{13}]_3 = \boldsymbol{T}_{013}\boldsymbol{R}_3. \tag{71}$$

Rigid Body 14

The motion of this body is analyzed in $\mathcal{F}_3$. Similar to rigid body 13, the angular velocity of body 14 is

$$\boldsymbol{\omega}_{14} = \boldsymbol{\omega}_{13}. \tag{72}$$

The position vector $\boldsymbol{\xi}_{14}$ in $\mathcal{F}_3$ is

$$[\boldsymbol{\xi}_{14}]_3 = [\boldsymbol{\xi}_{\mathrm{b}3}]_3 + \frac{1}{2}([\boldsymbol{\xi}_{\mathrm{a}3}]_3 - [\boldsymbol{\xi}_{\mathrm{b}3}]_3) + \left[\frac{b-c}{2}, 0, 0\right]^{\mathrm{T}} + \left[\frac{d}{4} + l, \frac{d}{4}, 0\right]^{\mathrm{T}}$$
$$= \frac{1}{2}\begin{bmatrix} h\cos\alpha_5 + [x_{\mathrm{c}}]_3 + b - c + d/2 + 2l \\ h\sin\alpha_5 + [y_{\mathrm{c}}]_3 - \dfrac{\sqrt{3}}{6}(s+a) + d/2 \\ h\sin\alpha_5\sin\beta_3 + [z_{\mathrm{c}}]_3 \end{bmatrix}. \tag{73}$$

Therefore, the velocity of body 14 is

$$[\boldsymbol{v}_{14}]_3 = [\boldsymbol{v}_{13}]_3. \tag{74}$$

and the twist $\boldsymbol{t}_{14}$ and the TSM $\boldsymbol{T}_{14}$ of body 14 in $\mathcal{F}_3$ are

$$[\boldsymbol{t}_{14}]_3 = [\boldsymbol{t}_{13}]_3, \quad [\boldsymbol{T}_{14}]_2 = [\boldsymbol{T}_{13}]_3 = \boldsymbol{T}_{013}\boldsymbol{R}_3. \tag{75}$$

Rigid Body 15

The motion of this body is analyzed in $\mathcal{F}_3$. Similar to rigid body 7, the angles of rotation of body-15 are

$$\phi_{15} = \beta_3, \quad \theta_{15} = 0, \quad \psi_{15} = \alpha_5 - (\pi - \gamma). \tag{76}$$

The angular velocity of body 15 is

$$\boldsymbol{\omega}_{15} = \left[\dot{\phi}_{15}, \dot{\theta}_{15}, \dot{\psi}_{15}\right] = \left[\dot{\beta}_3, 0, \dot{\alpha}_5\right]^{\mathrm{T}}. \tag{77}$$

The position vector $\boldsymbol{\xi}_{15}$ derived from the geometric relation shown in Fig. 2 is given as

$$[\boldsymbol{\xi}_{15}]_3 = [\boldsymbol{\xi}_{\mathrm{s}3}]_3 + \frac{1}{2}([\boldsymbol{\xi}_{\mathrm{b}3}]_3 - [\boldsymbol{\xi}_{\mathrm{s}3}]_3) - \left[\frac{b-c}{2}, 0, 0\right]^{\mathrm{T}} + \left[\frac{d}{4} + l, -\frac{d}{4}, 0\right]^{\mathrm{T}}$$
$$= \frac{1}{2}\begin{bmatrix} h\cos\alpha_5 - b + c + d/2 + 2l \\ h\sin\alpha_5 - \dfrac{\sqrt{3}}{3}s - d/2 \\ h\sin\alpha_5\sin\beta_3 \end{bmatrix}. \tag{78}$$

Therefore, the velocity of body 15 is

$$[\boldsymbol{v}_{15}]_3 = [\dot{\boldsymbol{\xi}}_{15}]_3 = \frac{1}{2}\begin{bmatrix} -\dot{\alpha}_5 h\sin\alpha_5 \\ \dot{\alpha}_5 h\cos\alpha_5 \\ \dot{\alpha}_5 h\cos\alpha_5\sin\beta_3 + \dot{\beta}_3 h\sin\alpha_5\cos\beta_3 \end{bmatrix}, \tag{79}$$

and the twist $\boldsymbol{t}_{15}$ becomes

$$[\boldsymbol{t}_{15}]_3 = \begin{bmatrix} 0 & 0 & 1 \\ 0 & 0 & 0 \\ 1 & 0 & 0 \\ -\frac{1}{2}h\sin\alpha_5 & 0 & 0 \\ \frac{1}{2}h\cos\alpha_5 & 0 & 0 \end{bmatrix} \begin{bmatrix} \dot{\alpha}_5 \\ \dot{\alpha}_6 \\ \dot{\beta}_3 \end{bmatrix} = \boldsymbol{T}_{015}\dot{\boldsymbol{\alpha}}_3. \tag{80}$$

Hence, the TSM of body 15 in $\mathcal{F}_3$ is

$$[\boldsymbol{T}_{15}]_3 = \boldsymbol{T}_{015}\boldsymbol{R}_3. \tag{81}$$

Rigid Body 16

Similar to rigid body 15, the angular velocity of rigid body 16 is

$$\boldsymbol{\omega}_{16} = \boldsymbol{\omega}_{15}. \tag{82}$$

The position vector $\boldsymbol{\xi}_{16}$ derived from the geometric relation shown in Fig. 2 is given as

$$\begin{aligned} [\boldsymbol{\xi}_{16}]_3 &= [\boldsymbol{\xi}_{s3}]_3 + \frac{1}{2}([\boldsymbol{\xi}_{b3}]_3 - [\boldsymbol{\xi}_{s3}]_3) + \left[\frac{b-c}{2}, 0, 0\right]^{\mathrm{T}} + \left[\frac{d}{4} + l, -\frac{d}{4}, 0\right]^{\mathrm{T}} \\ &= \frac{1}{2}\begin{bmatrix} h\cos\alpha_5 + b - c + d/2 + 2l \\ h\sin\alpha_5 - \dfrac{\sqrt{3}}{3}s - d/2 \\ h\sin\alpha_5\sin\beta_3 \end{bmatrix}. \end{aligned} \tag{83}$$

Therefore, the velocity of body 16 is

$$[\boldsymbol{v}_{16}]_3 = [\boldsymbol{v}_{15}]_3, \tag{84}$$

and the twist $\boldsymbol{t}_{16}$ and the TSM $\boldsymbol{T}_{16}$ of body 16 in $\mathcal{F}_3$ are

$$[\boldsymbol{t}_{16}]_3 = [\boldsymbol{t}_{15}]_3, \quad [\boldsymbol{T}_{16}]_3 = [\boldsymbol{T}_{15}]_3 = \boldsymbol{T}_{015}\boldsymbol{R}_3. \tag{85}$$

3 Dynamics

The mathematical model of the TBA under study is of the general form [12]:

$$\boldsymbol{M}\ddot{\boldsymbol{q}} + \boldsymbol{C}\dot{\boldsymbol{q}} + \boldsymbol{D}\dot{\boldsymbol{q}} + \boldsymbol{K}\boldsymbol{q} = \boldsymbol{\tau}, \tag{86}$$

where $\boldsymbol{M}$ is the 3×3 generalized inertia matrix, $\boldsymbol{C}$ the 3×3 generalized matrix of Coriolis and centrifugal forces, $\boldsymbol{D}$ the damping matrix, $\boldsymbol{K}$ the generalized stiffness matrix and $\boldsymbol{\tau}$ the vector of generalized force, all given below:

$$
\begin{aligned}
\boldsymbol{M} &\equiv \sum_{i=1}^{16} \boldsymbol{T}_i^{\mathrm{T}} \boldsymbol{M}_i \boldsymbol{T}_i, \quad \boldsymbol{C} \equiv \sum_{i=1}^{16} (\boldsymbol{T}_i^{\mathrm{T}} \boldsymbol{M}_i \dot{\boldsymbol{T}}_i + \boldsymbol{T}_i^{\mathrm{T}} \boldsymbol{W}_i \boldsymbol{M}_i \boldsymbol{T}_i), \\
\boldsymbol{K} &\equiv \sum_{i=1}^{16} \boldsymbol{T}_i^{\mathrm{T}} \boldsymbol{K}_i \boldsymbol{T}_i, \quad \boldsymbol{\tau} \equiv \sum_{i=1}^{16} \boldsymbol{T}_i^{T} \boldsymbol{w}_i, \quad \boldsymbol{W}_i \equiv \begin{bmatrix} \boldsymbol{\Omega}_i & \boldsymbol{0} \\ \boldsymbol{0} & \boldsymbol{0} \end{bmatrix},
\end{aligned}
\tag{87}
$$

where $\boldsymbol{M}_i$ is the 6×6 inertia dyad [12] of ith rigid body; $\boldsymbol{W}_i$ is the 6×6 angular velocity *dyad* of the ith rigid body, corresponding to the twist $\boldsymbol{t}_i$; $\boldsymbol{K}_i$ is the 6×6 stiffness matrix of the elastic feet attached to the ith rigid body; $\boldsymbol{w}_i$ is the wrench acting on the ith body; and $\boldsymbol{\Omega}_i$ is the 3×3 cross-product matrix[1] of the angular-velocity vector $\boldsymbol{\omega}_i$ of the ith rigid body.

The expression of the generalized stiffness matrix $\boldsymbol{K}$ in Eq. (87) is derived based on the assumption of small-amplitude rotations of the limbs. By multiplying both sides of Eq. (2) by the time increment Δt, the pose increment of the ith leg can be represented as a linear transformation given by $\boldsymbol{T}_i$ of the increment of the independent generalized position vector.

The stiffness matrix of the limbs with two feet can be expressed as

$$
\boldsymbol{K}_i = \mathrm{diag}(k_{\mathrm{out}}, 0, k_{\mathrm{in}}, 0, 0, 0), \ i = 5, 6, \ldots, 16, \tag{88}
$$

where k_{in} and k_{out} are, respectively, the in-plane and the out-of-plane stiffness coefficients of a leg with two feet, which compose the generalized stiffness matrix of the TBA system.

Linear damping from the Rayleigh dissipation function is used for the TBA damping model, denoted by the damping matrix $\boldsymbol{D}$. It is assumed that all damping comes from air drag within the gap between the proof-mass and the handle wafer; two major types of damping that occur in the micro-scale TBA are slide-film and squeezed-film damping [1, 2].

4 Modal Analysis

4.1 Parameters

Here we derive the expressions for the inertia parameters of the rigid bodies. In the X-Y plane, the bar-shaped rigid bodies are basically parallelepipeds, the limbs parallelograms and the proof-mass an equilateral triangular prism. The mass of each bar, proof-mass, leg, and the moment of inertia of each bar and leg are expressed in terms of the structural parameters, namely

$$
\begin{aligned}
&m_{\mathrm{bar}} = \rho b d w, \quad m_{\mathrm{pm}} = \frac{\sqrt{3}}{4} \rho a^2 w, \quad m_{\mathrm{leg}} = \frac{\sqrt{2}}{2} \rho e c w, \quad I_{\mathrm{barx}} = \frac{1}{12} m_{\mathrm{bar}} \left(d^2 + w^2\right), \\
&I_{\mathrm{legx}} = \frac{1}{12} m_{\mathrm{leg}} \left(e^2 + w^2\right), \quad I_{\mathrm{legy}} = \frac{1}{12} m_{\mathrm{leg}} \left(w^2 + c^2\right), \quad I_{\mathrm{legz}} = \frac{1}{12} m_{\mathrm{leg}} \left(e^2 + c^2\right).
\end{aligned}
\tag{89}
$$

where ρ is the material density; $I_{\mathrm{leg}x}$, $I_{\mathrm{leg}y}$, $I_{\mathrm{leg}z}$ are defined around the limb-central line along the width, length, and depth sides, respectively; $I_{\mathrm{bar}x}$ is defined around the bar-central line along the length side. The moments of inertia will be transformed into the local frames with respect to the

[1] This means that $\boldsymbol{\Omega}_i \boldsymbol{p} \equiv \boldsymbol{\omega}_i \times \boldsymbol{p}$, for any $\boldsymbol{p} \in \mathbb{R}^3$.

angle γ of the limbs. Other moments of inertia of the proof-mass and the bar-shaped rigid bodies need not be expressed explicitly because they undergo pure translation.

The overall stiffness of the TBA depends on the generalized stiffness of each leg with two feet, a good estimation of which is obtained from the smallest stiffnesses among the six stiffnesses: bending, shearing and torsional stiffness of leg and foot. For example, for the in-plane motion, the bending stiffness of the foot $k_{z\mathrm{fb}}$ is one order of magnitude smaller than the others; therefore, the in-plane stiffness coefficient k_{in} is found based on the bending stiffness of the foot. By the same token, the out-of-plane stiffness coefficient k_{out} is found based on the torsional stiffnesses of the leg ,$k_{x\mathrm{lt}}$, and the foot $k_{x\mathrm{ft}}$, since they are generally smaller for the out-of-plane motion. With the two feet working as torsional springs in parallel around the Z-axis and in series around the X-axis, the stiffnesses k_{in} and k_{out} are derived as

$$k_{\mathrm{in}} = 2k_{z\mathrm{fb}} = \frac{Ewt_{\mathrm{m}}^3}{2l}, \quad k_{\mathrm{out}} = \frac{1}{\frac{1}{k_{x\mathrm{ft}}/2} - \frac{1}{k_{x\mathrm{lt}}}} = \frac{12Ew^3ct_{\mathrm{m}}}{2lc - \sqrt{2}et_{\mathrm{m}}}. \tag{90}$$

4.2 Model Linearization

We linearize the inertia matrix $\boldsymbol{M}(\boldsymbol{\alpha})$ and the stiffness matrix $\boldsymbol{K}(\boldsymbol{\alpha})$ from the assumption of small-amplitude rotations of the limbs, so that estimates of the natural frequencies of the undamped TBA system will be available. The value of $\boldsymbol{\alpha}$ at the home posture is defined as $\alpha_1^0 = \alpha_3^0 = \alpha_5^0 = 3\pi/4$, $\alpha_2^0 = \alpha_4^0 = \alpha_6^0 = \pi/4$ and $\beta_1^0 = \beta_2^0 = \beta_3^0 = 0$. Substituting these values into the TSMs, the generalized inertia and stiffness matrices become

$$\boldsymbol{M}_{\mathrm{e}} = \begin{bmatrix} M_{\mathrm{in}}\mathbf{1}_{2\times 2} & \mathbf{0}_2 \\ \mathbf{0}_2^T & M_{\mathrm{out}} \end{bmatrix}, \quad \boldsymbol{K}_{\mathrm{e}} = \begin{bmatrix} K_{\mathrm{in}}\mathbf{1}_{2\times 2} & \mathbf{0}_2 \\ \mathbf{0}_2^T & K_{\mathrm{out}} \end{bmatrix}, \tag{91}$$

where $\mathbf{0}_2$ denotes the 2-dimensional zero vector; the in-plane entries M_{in}, K_{in} and the out-of-plane entries M_{out}, K_{out} for the translational motion of the proof-mass are

$$\begin{aligned} M_{\mathrm{in}} &= m_{\mathrm{pm}} + \frac{3m_{\mathrm{bar}}}{2} + \frac{9m_{\mathrm{leg}}}{2} + \frac{6I_{\mathrm{leg}z}}{h^2}, \quad K_{\mathrm{in}} = \frac{6k_{\mathrm{in}}}{h^2}, \\ M_{\mathrm{out}} &= m_{\mathrm{pm}} + \frac{3}{4}m_{\mathrm{bar}} + \frac{15}{4}m_{\mathrm{leg}} + \frac{3(I_{\mathrm{leg}x} + I_{\mathrm{leg}y})}{h^2} + \frac{3I_{\mathrm{bar}x}}{2h^2}, \quad K_{\mathrm{out}} = \frac{6k_{\mathrm{out}}}{h^2}. \end{aligned} \tag{92}$$

Moreover, m_{pm}, m_{bar}, m_{leg} are, respectively, the masses of: the proof-mass, the bars, and the limbs; $I_{\mathrm{leg}x}$, $I_{\mathrm{leg}y}$, $I_{\mathrm{leg}z}$ are the moments of inertia of the limbs around their central line: along the width side, the length side, and the depth side, respectively; $I_{\mathrm{bar}x}$ is the moment of inertia of the bars around their central line along the length side. Hence, all moments of inertia are defined at the c.o.m.

The matrix of generalized Coriolis and centrifugal forces $\boldsymbol{C}(\boldsymbol{\alpha})$ takes the form

$$\boldsymbol{C}_{\mathrm{e}} = \begin{bmatrix} C_{11} & C_{12} & 0 \\ C_{12} & -C_{11} & 0 \\ 0 & 0 & 0 \end{bmatrix}, \tag{93}$$

where

$$C_{11} = c_1\dot{x}_{\rm c} - c_2\dot{y}_{\rm c}, \quad C_{12} = -c_2\dot{x}_{\rm c} - c_1\dot{y}_{\rm c},$$
$$c_1 = \frac{3}{8}\frac{\sqrt{2}(m_{\rm bar}+2m_{\rm leg})}{h}, \quad c_2 = \frac{3}{8}\frac{\sqrt{2}(m_{\rm bar}+m_{\rm leg})}{h} + \frac{3}{2}\frac{\sqrt{2}I_{\rm legz}}{h^3}.$$

Matrix $\boldsymbol{C}_{\rm e}$ is negligible when compared with other terms in Eq. (86), which will be explained later in Section 5.

To analyze the natural frequency of the undamped TBA system in Eq. (86), the *positive-definite square root* [12] of $\boldsymbol{M}_{\rm e}$, represented as $\boldsymbol{N}_{\rm e} \equiv \sqrt{\boldsymbol{M}_{\rm e}}$, will be used. Then, the frequency matrix $\boldsymbol{\Lambda}$ and the natural-frequency array $\boldsymbol{\omega}$ of the system are

$$\boldsymbol{\Lambda} \equiv \sqrt{\boldsymbol{N}_{\rm e}^{-1}\boldsymbol{K}_{\rm e}\boldsymbol{N}_{\rm e}^{-1}}, \quad \boldsymbol{\omega} \equiv {\rm eig}(\boldsymbol{\Lambda}) = [\omega_{\rm in}, \omega_{\rm in}, \omega_{\rm out}]^T, \tag{94}$$

where ${\rm eig}(\cdot)$ denotes the array of eigenvalues of matrix $(\cdot)$. Moreover, $\omega_{\rm in}$ and $\omega_{\rm out}$ can be derived as

$$\omega_{\rm in} = \frac{2\sqrt{3}\sqrt{k_{\rm in}}}{\sqrt{2h^2m_{\rm pm} + 3h^2m_{\rm bar} + 9h^2m_{\rm leg} + 12I_{{\rm leg}z}}},$$
$$\omega_{\rm out} = \frac{2\sqrt{6}\sqrt{k_{\rm out}}}{\sqrt{4h^2m_{\rm pm} + 3h^2m_{\rm bar} + 15h^2m_{\rm leg} + 12I_{{\rm leg}x} + 12I_{{\rm leg}y} + 6I_{{\rm bar}x}}}.$$

The inertia matrix $\boldsymbol{M}_{\rm e}$ in Eq. (91) and the natural-frequency vector $\boldsymbol{\omega}$ in Eq. (94) are regarded as accuracy indices of the parametric mathematical model, compared with the FEA results.

5 FE validation

5.1 SBA MEMS Prototype

Since the SBA can be regarded as an implementation of the TBA, the parameters of the SBA MEMS prototype [2] are listed in Table 1 for validation of the mathematical model.

Table 1: Parameters of the SBA MEMS prototype

Parameter	a	s	e	b	c	d	$t_{\rm m}$	l	w	γ	E (Pa)	ν (Kg/m^3)	ρ
Value (μm)	3333	10398	700	1400	200	210	20	210	300	$\pi/4$	1.618×10^{11}	0.222	2330

Combined with the expressions of the structure parameters in the section of Modal Analysis, the generalized inertia matrix $\boldsymbol{M}_{\rm e}$ and the generalized stiffness $\boldsymbol{K}_{\rm e}$ in Eq. (91) are computed based on the numerical values of the parameters given below:

$$\begin{aligned} M_{\rm in}^{\rm mems} &= 3.9909\times10^{-6}\ ({\rm Kg}), \quad K_{\rm in}^{\rm mems} = 5334.7\ ({\rm N/m});\\ M_{\rm out}^{\rm mems} &= 3.7836\times10^{-6}\ ({\rm Kg}), \quad K_{\rm out}^{\rm mems} = 25492\ ({\rm N/m}). \end{aligned} \tag{95}$$

Then, the natural frequency in Eq. (94) of the TBA prototype is given by

$$\begin{aligned} \omega_{\text{in}}^{\text{mems}} &= 36561 \text{ (rad/s)}, \quad \text{f}_{\text{in}}^{\text{mems}} = \frac{\omega_{\text{n}}}{2\pi} = 5818.9 \text{ (Hz)}, \\ \omega_{\text{out}}^{\text{mems}} &= 82083 \text{ (rad/s)}, \quad \text{f}_{\text{out}}^{\text{mems}} = \frac{\omega_{\text{n}}}{2\pi} = 13064 \text{ (Hz)}. \end{aligned} \tag{96}$$

We now compare the static response and the natural frequency of the SBA from the NOC modelling with the FEA results from ANSYS.

To obtain the generalized stiffness matrix of the accelerometer, the forces are applied only at the c.o.m. of the proof-mass. The stiffness and the frequency matrices from FEA [2] are

$$\boldsymbol{K}_{\text{fea}}^{\text{mems}} = \text{diag}(5581.9, 5580.7, 25065.2) \text{ (N/m)}, \quad \text{f}_{\text{fea}}^{\text{mems}} = [5858.3, 5859.1, 12890]^{\text{T}} \text{ (Hz)}, \tag{97}$$

which produce the generalized inertia matrix

$$\boldsymbol{M}_{\text{fea}}^{\text{mems}} = \text{diag}(4.1198, 4.1178, 3.8213) \times 10^{-6} \text{ (Kg)}. \tag{98}$$

The Bode plots of in-plane and out-of-plane frequency responses are shown in Figs. 3(a) and (b), respectively, for comparison of the NOC analysis with the FEA results of the linearized undamped SBA system.

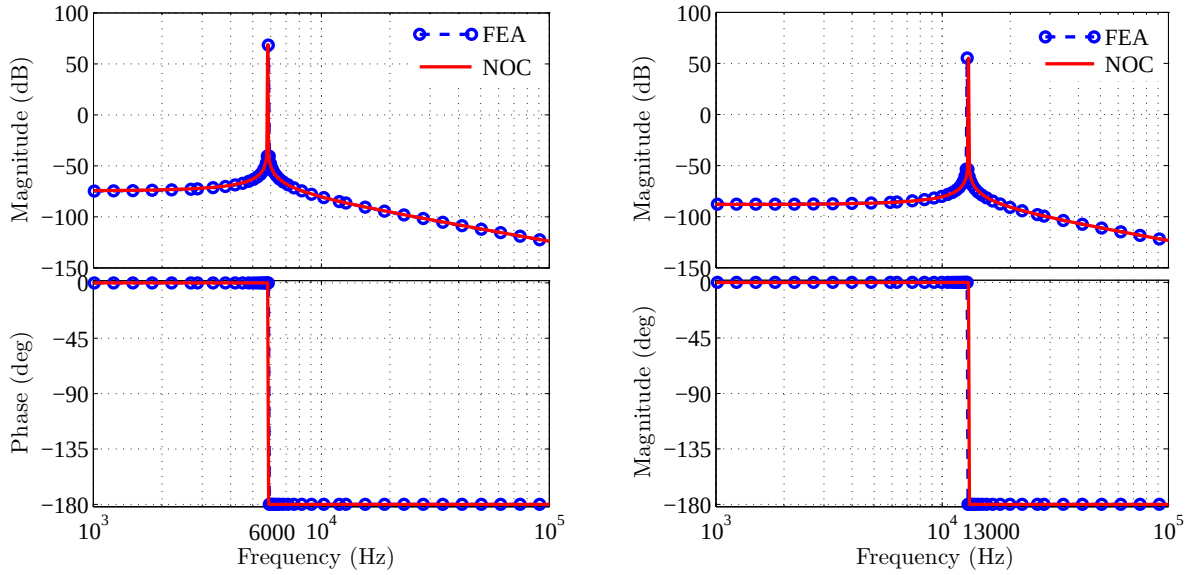

Figure 3: Bode plots of the NOC and FEA results of the MEMS prototype: (a) in-plane; (b) out-of-plane

By comparing the inertia matrices in Eqs. (95) and (98), the percentage errors[2] turn out to be $\{3.13\%, 3.18\%, 0.99\%\}$, respectively, for the in-plane and out-of-plane motion. For comparison, the

[2](paramatric value−numerical value)/numerical value ×100%

corresponding percentage errors without Lamé Curves are $\{2.41\%, 2.43\%, 1.10\%\}$, respectively. By the same token, comparing the vector of the natural frequency in Eqs. (96) and (97), the percentage errors are $\{0.673\%, 0.686\%, 1.35\%\}$, respectively, for the in-plane and out-of-plane motion.

5.2 Optimum TBA

It should be noted that this mathematical model is valid for TBAs of all sizes, which is shown by a set of non-proportional dimensions optimized for the largest frequency ratio between the non-sensitive and sensitive directions. In addition, the feet of the TBA, the thinnest component in the architecture, is constrained to be above 25 μm to avoid fracture during micro-fabrication, according to our experience. The thickness of the TBA is fixed according to the silicon wafer. The results of the dimensional optimization are low-pass filtered thereafter to derive the natural frequencies in the hecto-Hertz bandwidth.

Since the lowest non-sensitive motion is always the out-of-plane translation, the frequency ratio f_3/f_1 between the out-of-plane and in-plane translations is monitored specially. The sensitivity of the frequency ratios to the design parameters is shown in Fig. 4, in which the frequency ratio f_3/f_1 is inversely proportional to all the design parameters, except for the lengths b and e of the bar and the limb, respectively.

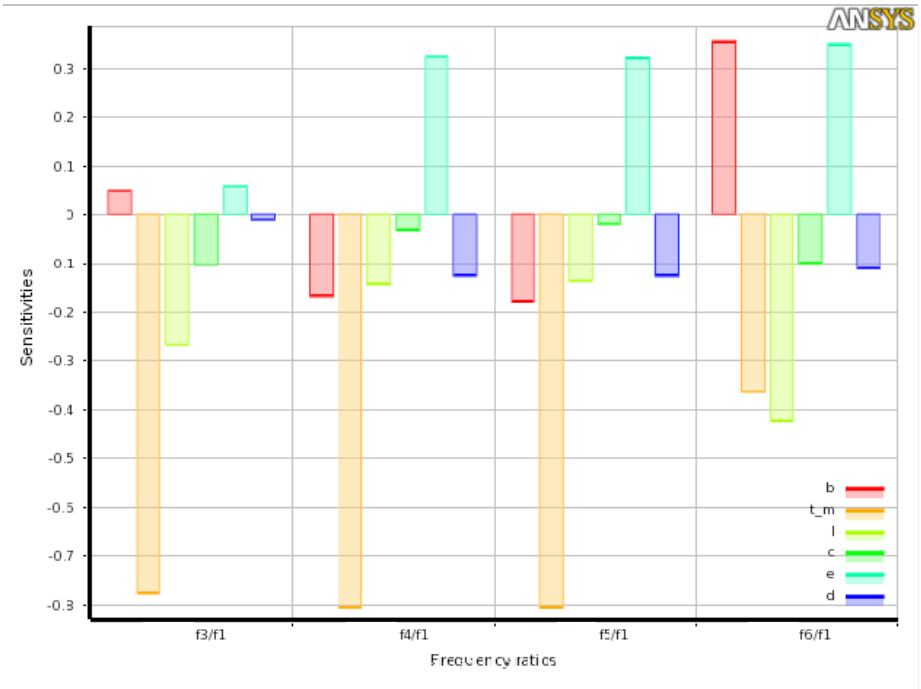

Figure 4: Sensitivity of the frequency ratios to the design parameters

It is shown that the frequency ratio f_3/f_1 is most sensitive to the width t_{m} of the feet. The other variable of the feet dimensions, length l, is the second influential parameter, with around one third of the width influence. The sensitivity f_3/f_1 to other design parameters is smaller than 15% of the foot width.

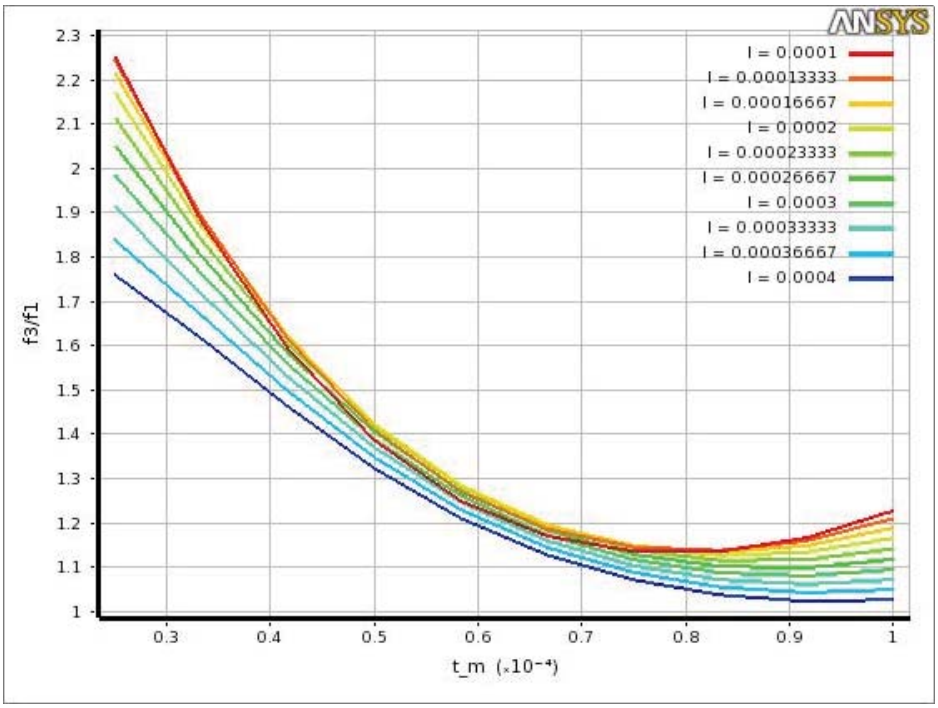

Figure 5: Frequency ratio f_3/f_1 w.r.t. the feet width t_m and length l

Given that the dimensions of the feet matter most regarding the frequency ratio f_3/f_1, its response chart with respect to the width t_m and the length l of the feet is illustrated in Fig. 5. Obviously, the frequency ratio f_3/f_1 reaches its peak when t_m and l are all smallest within their design range. However, this has to be compromised, considering the manufacturing feasibility and the safety in operation. Therefore, a second round of dimensional optimization is conducted around a narrower range of the design parameters, but with $t_\mathrm{m} = 30$ μm and $b = 4$ mm fixed for manufacturing safety and size control.

The preliminary results of optimum dimensions are listed in Table 2 for further validation of the applicability of the mathematical model.

Table 2: Optimum parameters of the TBA

Parameter	a	s	e	b	c	d	t_m	l	w
Value (10^{-6} m)	12000	28383	2931.5	4000	749.22	207.47	30	94.051	300

The frequency ratio f_3/f_1, after optimization, is 2.90 under the aspect ratio of $w/t_\mathrm{m} = 10$, while the frequency ratio in Eq. (97) is 2.20 under the aspect ratio of 15. The aspect ratio decreases by 33.3%, while the frequency ratio increases by 31.8%. Since the frequency ratio is identical to the aspect ratio for a single-dof suspension, the change of frequency ratio of the biaxial TBA will be compared with the change of the aspect ratio. In this sense, the frequency ratio increased by 65.2%.

The FEA results of the stiffness matrix and the frequency vector are

$$\boldsymbol{K}_{\text{fea}}^{\text{opt}} = \text{diag}(1530.3, 1531.5, 12333) \text{ N/m}, \quad \text{f}_{\text{fea}}^{\text{opt}} = [879.7, 880.22, 2554.4]^{\text{T}} \text{ Hz}, \tag{99}$$

which produce the inertia matrix

$$\boldsymbol{M}_{\text{fea}}^{\text{opt}} = \text{diag}(5.0090, 5.0070, 4.7876) \times 10^{-5} \text{ Kg}. \tag{100}$$

The corresponding inertia matrix from Eq. (95) is

$$\boldsymbol{M}_{\text{mth}}^{\text{opt}} = \text{diag}(4.9948, 4.9948, 4.8400) \times 10^{-5} \text{ Kg}. \tag{101}$$

The percentage errors of the inertia matrix are $\{0.283\%, 0.244\%, 1.09\%\}$, respectively, for the in-plane and out-of-plane motion. The percentage errors are at the same level as those in Subsection 5.1; the mathematical model is thus effective and stable for the TBA architecture.

The matrix of Coriolis and centrifugal forces is not simulated in the FEA, since $\boldsymbol{C}(\boldsymbol{\alpha}, \dot{\boldsymbol{q}})$ is small[3] as compared with other terms in Eq. (86). Taking the optimum dimensions for example, the coefficients c_1 and c_2 become 4.5353×10^{-4} Kg/m and 3.2835×10^{-4} Kg/m, respectively. The displacement under an acceleration of $10g$ in the x-axis is approximately $x_{\text{c}} = 3.2110 \times 10^{-6}$ m, and the maximum velocity is approximately $\dot{x}_{\text{c}} = \ddot{x}_{\text{c}} x_{\text{c}}/2 = 2.5100 \times 10^{-2}$ m/s. In this case, the term $c_1 \dot{x}_{\text{c}}$ is in the order of 10^{-6} N, three orders of magnitude lower than the inertia and the elastic forces. Therefore, the Coriolis and centrifugal terms are negligible.

5.3 Rapid Prototype

A scaled-up prototype produced by 3D printing was used for experimental validation of the mathematical model. Because of the limitation of the vibration-measurement system[4], only the in-plane responses were tested.

The values of the geometric parameters of the rapid prototype are listed in Table 3.

Table 3: Geometric parameters of the TBA rapid prototype

Parameter	a	s	e	b	c	d	t_{m}	l	w
Value (mm)	80	24.96	16.79	35.12	8.72	5.04	2	5.04	13

As to the material properties, the Young modulus, Poisson ratio and density are not provided directly from the data sheet[5] for the composed digital material used for the rapid prototype. According to the data sheet, one of the primary materials is a rigid opaque material "VeroWhitePlus RGH835", which has a density of 1170-1180 Kg/m^3 and a Young modulus of 2-3 GPa. The other is a rubber-like material "TangoBlackPlus FLX980/TangoPlus FLX930", which has a density of

[3]Comparison is based in the matrix Frobenius norm

[4]The Modal Shop 2100E11

[5]http://www.stratasys.com/materials/material-safety-data-sheets/polyjet/~/media/Main/Secure/Material%20Specs%20MS/PolyJet-Material-Specs/PolyJet_Materials_Data_Sheet.ashx

1170-1180 Kg/m^3 and an uncertain Young modulus, estimated to be 0.01-0.1 GPa, like rubber. The Poisson ratio is presumed to be 0.3 and the proportion of the two materials to be half and half. Therefore, a rough estimation of material properties is obtained by averaging the density and Young modulus of the two primary materials. As a result, the Young modulus of the material is $E = 1.275 \times 10^{11}$ Pa, the Poisson ratio $\nu = 0.3$ and the density of the material $\rho = 1150$ Kg/m^3.

Combined with the parameters in Section 4.1, the evaluated entry of the generalized inertia M_{in} and the evaluated entry of the generalized stiffness K_{in} in Eq. (91) are given by

$$M_{\text{mth}}^{\text{rap}} = 5.2596 \times 10^{-2}\ (\text{Kg} \cdot \text{m}^2), \quad K_{\text{mth}}^{\text{rap}} = 131711\ (\text{N} \cdot \text{m/rad}) \tag{102}$$

Then, the in-plane natural frequency in Eq. (94) of the TBA prototype is

$$\omega_{\text{mth}}^{\text{rap}} = 1582.4\ (\text{rad/s}), \quad \text{f}_{\text{mth}}^{\text{rap}} = \frac{\omega_{\text{n}}}{2\pi} = 251.84\ (\text{Hz}) \tag{103}$$

The displacement of the centre of the proof-mass under a 1-N force along any direction is about 3.8297×10^{-6} m, while the result from the generalized stiffness matrix in Eq. (102) is 3.8721×10^{-6} m, with an error of 1.1%. The natural frequency by FEA is $f_{\text{fea}}^{\text{rap}} = 250.34$ Hz, while the NOC result is $f_{\text{mth}}^{\text{rap}} = 251.84$ Hz in Eq. (103), with an error of 0.60%.

The rapid prototype was tested on the vibration devices, as shown in Fig. 6. The frequency range of the vibration test is 10-300 Hz with a step of 10 Hz.

(a) (b)

Figure 6: Vibration test of the rapid prototype: (a) rapid prototype; (b) vibration devices

The dynamic response of the rapid prototype is obtained from the vibration tests for different orientations. The Bode plots are depicted in Fig. 7 for two arbitrary vertices of the prototype frame. At low frequencies, the signal-to-noise ratio is so low that the corresponding plots are not reliable. However, an obvious peak can be observed as the fundamental resonance frequency, estimated to be $f_{\text{test}}^{\text{rap}} = 255$ Hz.

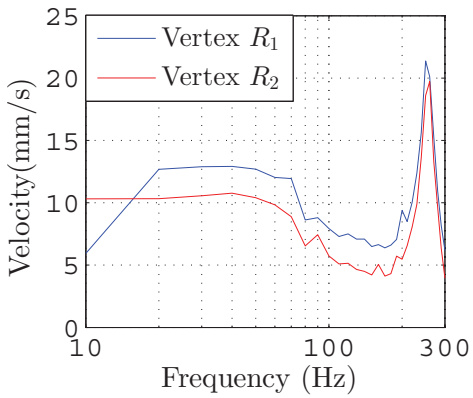

Figure 7: Test results of the frequencies

The fundamental frequencies of the rapid prototype are $f_{\text{mth}}^{\text{rap}} = 251.84$ Hz, $f_{\text{fea}}^{\text{rap}} = 250.47$ Hz and $f_{\text{test}}^{\text{rap}} = 255$ Hz, respectively, from the NOC model, FEA and tests. The three results are compatible, the percentage error between the NOC model and test results being 1.38%.

6 Conclusions

The static response and the natural frequency from the numerical FEA and the parametric NOC model are comparable, which reveals the feasibility and effectiveness of the proposed NOC model. The NOC model of the TBA offers insight into its dynamic behaviour under acceleration fields and can facilitate the control algorithm design for the closed-loop navigation system. The inertia and the stiffness matrices are *isotropic* in the plane of the proof-mass; therefore, the TBA motion in the sensitive axes can be modelled as a 1-dof system.

The isotropic structure allows us to extend the kinematic relations from one limb to the whole TBA by coordinate transformations. In this vein, it is convenient to model other regular polygonal structures from the TSMs derived here. Within the NOC, matrices are additive; additionally, the matrices are identical for the parallel limbs in each ΠΠ-limb. Hence, the modelling of alternative structures with different numbers of limbs in each ΠΠ-limb would be simplified.

The dimensional optimization of the TBA structure leads to a higher frequency ratio for a lower aspect ratio. The sensitivity analysis provides insight into the relation between the frequency ratios and the dimensions of the structure. The optimum dimensions from the dimensional optimization validate the mathematical model of the TBA architecture.

The vibration tests of the scaled-up rapid prototype provide the actual fundamental frequency in the sensitive plane of the accelerometer. Both the NOC and the FEA results are verified by physical tests, which validates the pertinence of the mathematical model.

References

[1] Cardou, F. *Design of Multiaxial Accelerometers with Simplicial Architectures for Rigid-Body Pose-and-Twist Estimation.* Ph.D. thesis, Department of Mechanical Engineering and Centre for Intelligent Machines, McGill University, Montreal, 2007.

[2] Zou, T. *Design of Biaxial Accelerometers for Rigid-Body Pose-and-Twist Estimation.* Ph.D. thesis, Department of Mechanical Engineering, McGill University, Montreal, 2013.

[3] Howell, L.L. *Compliant Mechanisms.* Wiley-Interscience, 2001.

[4] Wohlhart, K. "Der homogene paralleltrieb-mechanismus." *Mathematica Pannonica*, Vol. 2, No. 2, pp. 59 – 76, 1991.

[5] Wohlhart, K. "Displacement analysis of the general spatial parallelogram manipulator." pp. 104 – 111. *Proc. 3rd International Workshop on Advances in Robot Kinematics*, Ferrara, Italy, 1992.

[6] Wohlhart, K. "Inverse kinematics of manipulators with 3 revolute and 3 parallelogram joints." Vol. 45, pp. 35 – 40. *Proc. ASME 22nd. Biennial Mechanisms Conference*, Sept.13-16, Scottsdale, 1992.

[7] Hervé, J. and Sparacino, F. "Star, a new concept in robotics." pp. 176–183. *Proc. 3rd Int. Workshop on Advances in Robot Kinematics*, Sept.7-9, Ferrara, 1992.

[8] Desrochers, S. *Optimum Design of Simplicial Uniaxial Accelerometers.* Master's thesis, Department of Mechanical Engineering and Centre for Intelligent Machines, McGill University, Montreal, 2009.

[9] Angeles, J. *Fundamentals of Robotic Mechanical Systems: Theory, Methods, and Algorithms.* Third ed.. Springer, New York, NY, 2007.

[10] Jalón, J. and Bayo, E. *Kinematic and Dynamic Simulation of Multibody Systems-The Real-Time Challenge.* Springer-Verlag, 2009.

[11] Garneau, Y. and Angeles, J., S.A. *The Control of a Mobile Robot with Dual Wheel Transmission.* Technical Report TR-CIM-10-25, Department of Mechanical Engineering and Centre for Intelligent Machines, McGill University, Montreal, 2012.

[12] Angeles, J. *Dynamic Response of Linear Mechanical Systems: Modeling, Analysis and Simulation.* Springer, New York, NY, 2011.